Supplementary information

Microcavity Supported Lipid Membranes: Versatile Platforms for Building Asymmetric Lipid Bilayers and for Protein Recognition

*Guilherme B. Berselli[1], Nirod Kumar Sarangi[1], Sivaramakrishnan Ramadurai[1], Paul V. Murphy[2], Tia E. Keyes[1]**

[1]School of Chemical Sciences and National Centre for Sensor Research, Dublin City University, Dublin 9, Ireland

[2]School of Chemistry NUI Galway University Road, Galway Ireland.

AUTHOR INFORMATION

Corresponding author:

**E-mail: tia.keyes@dcu.ie*

Fabrication of gold microcavity array electrodes:

Figure S1 represents step by step the procedure for gold microcavity array fabrication. In step-1, 1μm sphere PS (1 wt% v/v in milli-Q water) was self-assembled on plasma treated gold substrate using drop-cast approach. After evaporation of water (Figure S1a) in step-2, the electrode was subjected to gold deposition by submerging the electrode into electroplating solution. The growth was monitored until the film grown up to half of the PS sphere diameter in between the intestinal space of PS sphere and stopped (Figure S1b). In step-3, the electrode was washed with Milli-Q water, dried under N_2 gas and submerged in a 1mM ethanolic solution of 6-mercapto-1-hexanol (SH) and kept for the formation of self-assembled monolayer. After 2 days, the electrode was removed from thiol solution and washed gently with ethanol to remove excess unbound thiol. In step-4 the substrate was dipped in THF solution for 10 min. In this process, the PS is removed and the microcavity array is formed (Figure S1c). The substrate was kept in PBS buffer

for more than 1 hr and ready for further use. Briefly, 1μm sphere PS (1 wt% v/v in milli-Q water) was self-assembled on plasma treated gold substrate using drop-cast approach. After evaporation of water (Figure S1a), the electrode was subjected to gold deposition by submerging the electrode into electroplating solutions. The growth was monitored using controlled potential deposition until the film has grown up to half of the PS sphere diameter in between the intestinal space of PS sphere and stopped (Figure S1b). Selective SAM formation at the top interface of the array was achieved by submerging the gold substrates in a 1 mM ethanolic solution of MH prior to the removal of the 1 μm polystyrene (PS) templating spheres. As described previously, the PS spheres could prevent the MH SAM forming at the pore interior, limiting the SAM to the interstitial planar regions at the top surface of the array between pores[1,2]. The chemical modification of MH treatment step improves the stability of the bilayer due to strong wettability of gold substrate with –OH functionalized interface. Next, the PS spheres were removed by submerging the gold substrate in THF for 10 min to form hemisphere microcavity arrays. As described previously, this step does not remove the SAM from the top surface and this further confirmed from EIS data (*vide supra*).[3]

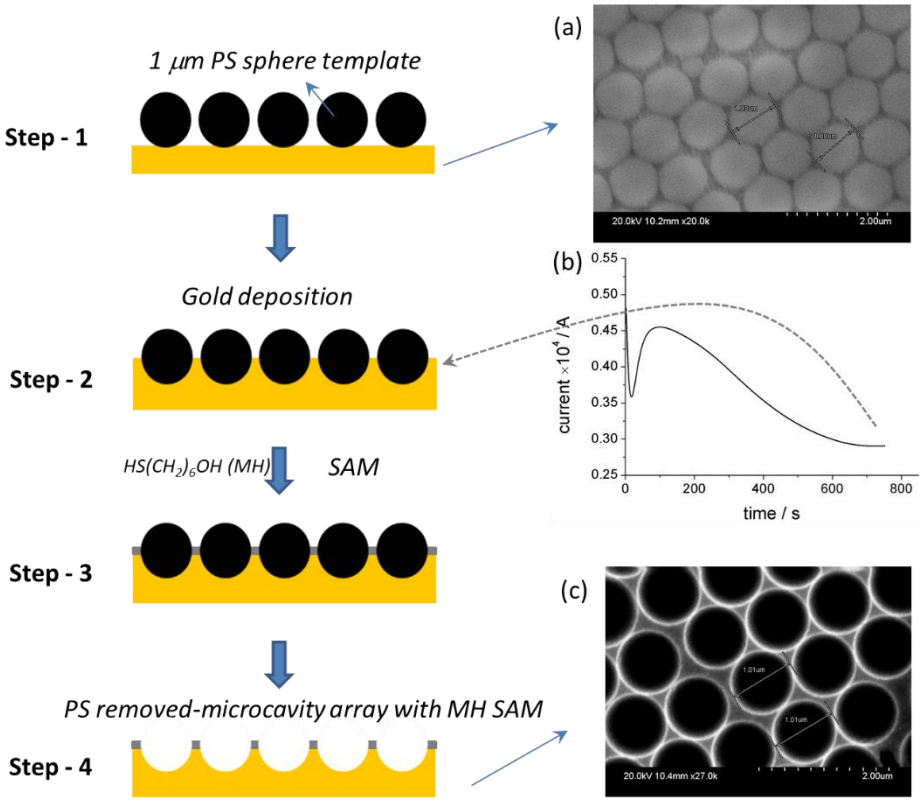

Figure S1. Schematic illustrations of step by step procedure for the fabrication of hemisphere microcavity array on gold substrate. (a) SEM image of PS sphere before gold deposition. (b) Represents the current-time curve during the electrodeposition of gold solution at -0.6 V vs Ag/AgCl. (c) Represents SEM image after PS removal. The scale bar of each image was 2 μm.

Fabrication of PDMS microcavity array

Figure S2 represents stepwise the procedure for the fabrication of microcavity array in PDMS substrate. Similarly, for gold electrodes preparation, in step-1 approximately 50 μL of 4.61 μm polystyrene spheres (0.1 wt% v/v in ethanol) was self-assembled on 1 cm x 1 cm fresh cleaved mica sheet. The PDMS mixture (10:1 ratio) is degassed in a vacuum chamber for 30 min and the bubble-free mixture is poured into a handmade aluminum mould to be cured at 90°C for 30 minutes. After curing, PS spheres were removed by sonicating the substrates in THF for 15 minutes and leftover for solvent evaporation in fume hood overnight.

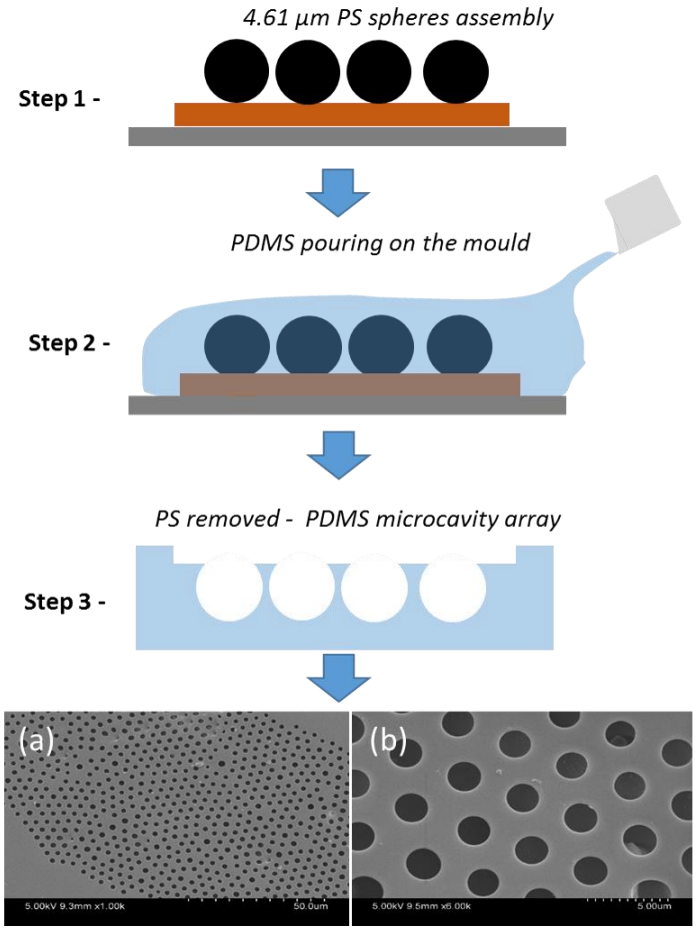

Figure S2. Schematic illustrations of step by step procedure for the fabrication of microcavity array on PDMS substrate. (a) and (b) SEM images of PDMS substrate after PS spheres removal. The scale bar of each image was 50µm and 5 µm, respectively.

Fluorescence Lifetime correlation spectroscopy (FLCS) calibration

The confocal volume was determined by prior calibration using Rhodamine 6G and Atto655, fitting the resulting autocorrelation function using the known diffusion coefficient of the dye at 20 °C. The free diffusion of the dyes in solution following the water viscosity correction expressed by equation (S1)[4] :

$$D(T) = D(25°C)\frac{T}{298.15K}\frac{8.9.10^{-4}\ Pa.s}{\eta(T)} \quad (S1)$$

Where D is the dye diffusion and η is the viscosity of water.

Lipid monolayer transfer using Langmuir-Blodgett films

Prior to filling the cavities with PBS buffer pH 7.4, the substrate is cleaned by oxygen plasma for 5 minutes and sonicated in PBS buffer for 1 hour. Usually, 50 µL of lipids (1 mg/ml in chloroform) is added drop by drop onto the subphase (MiliQ water, 18.2 MΩ.cm) at room temperature, and chloroform is allowed to evaporate for 10 min. The monolayers were with 4 cycles of compression/decompression at barrier speed of 20 mm/min at final surface pressure (Π) of 35 $mN.m^{-1}$. Then, the monolayer is compressed up to 32 $mN.m^{-1}$ and held for at least 300 s before transfer. Lipid monolayers were transferred onto to hydrophilic gold or PDMS substrates vertically at 5 and 10 mm/min at room temperature.

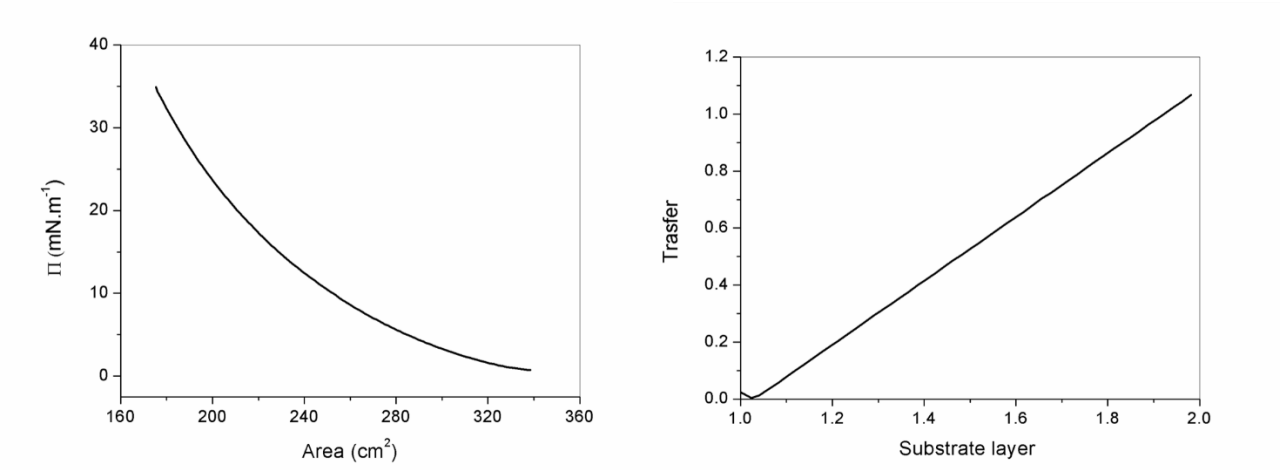

Figure S3. Lipid monolayer transfer using Langmuir-Blodgett lipid films. A typical DOPC isotherm (left) and transfer (right).

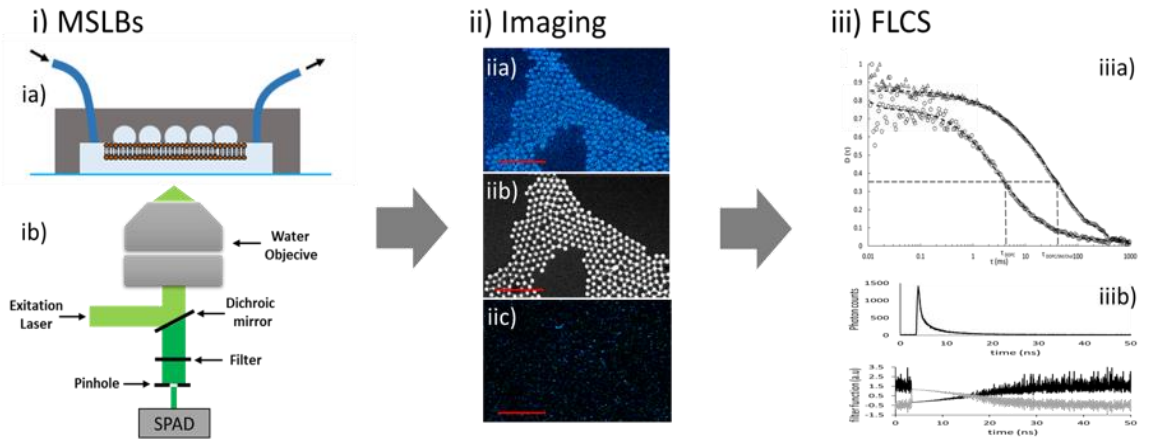
i) MSLBs
ia)
ib)
Water Objective
Exitation Laser
Dichroic mirror
Filter
Pinhole
SPAD
ii) Imaging
iia)
iib)
iic)
iii) FLCS
iiia)
iiib)
time (ns)

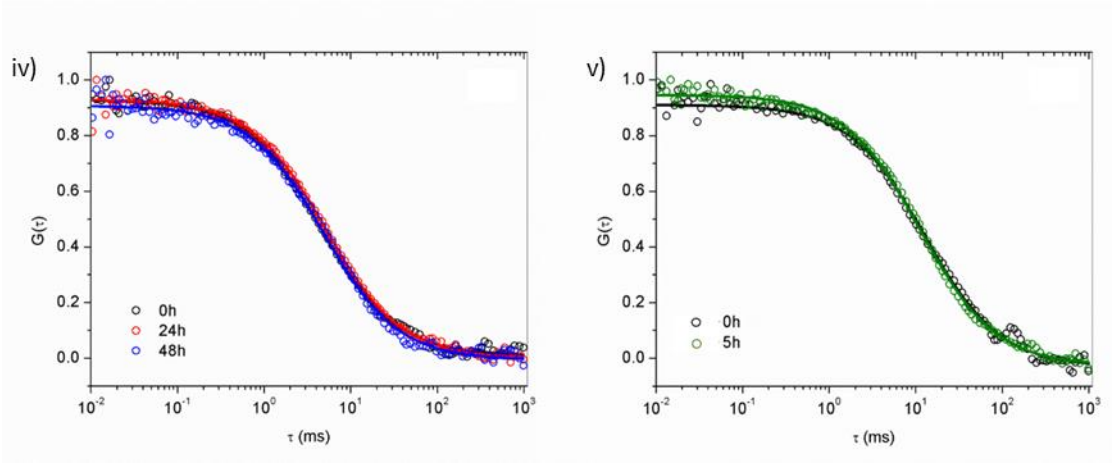
iv)
G(τ)
τ (ms)
0h
24h
48h
v)
0h
5h

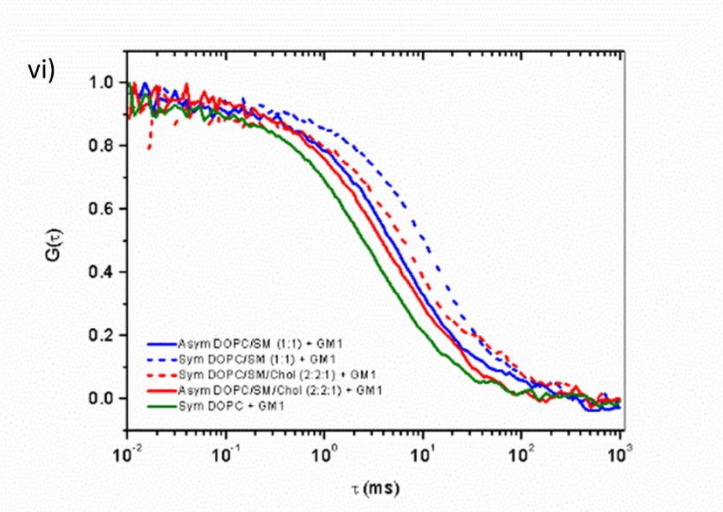
vi)
G(τ)
τ (ms)
Asym DOPC/SM (1:1) + GM1
Sym DOPC/SM (1:1) + GM1
Sym DOPC/SM/Chol (2:2:1) + GM1
Asym DOPC/SM/Chol (2:2:1) + GM1
Sym DOPC + GM1

Figure S4. Schematic illustrations of FCS measurement on buffer filled suspended lipid bilayers. (ia) and (ib) represents the MSLBs microcavity array mounted on a confocal microscope and the microscope apparatus used to excite the fluorophores (DOPE and CTb), respectively. (iia) represents fluorescence lifetime image obtained for DOPE-Atto655 on a DOPC/GM1 (1 mol%) lipid bilayer. (iib) shows the reflectance image obtained using and OD3 filter. (iic) shows the substrate exited with 532nm laser before incubation with CTb-A555 (no autofluorescence is observed). (iiia) and (iiib) shows the typical ACF curves obtained for DOPE and CTb for DOPC/GM1 (1 mol%) lipid bilayers and the filters used in fluorescence lifetime correlation spectroscopy. Lipid bilayer stability spanned over PDMS microcavity array: (iv) FLCS data obtained for a DOPC bilayer containing GM1 (1 mol%) in the distal leaflet. Initial measurement after sample preparation (black), after 24 hours (red) and after 48 hours (blue). (v) FLCS data obtained for an asymmetric lipid bilayer comprised of DOPC (proximal leaflet) and DOPC/SM (1:1) containing GM1 (1 mol%) in the distal leaflet after sample preparation (0 hour, black) and after 5 hours (green). The lines represent the fitting to the 2D diffusing model. (vi) FLCS DOPE-Atto655 autocorrelation curves (ACFs) obtained for asymmetric and symmetric lipid bilayers spanned over microcavities arrays.

Cholera Toxin Controls with lipid bilayers lacking GM1

The diffusion of CTb in solution was calculated by fitting the ACF (black open circles) displayed in Figure S4a using a pure free diffusional model and found to be around 54 ± 3 $\mu m^2.s^{-1}$. This value was used to estimate the pentameric radius of CTb (rCTb) using Stokes-Einstein relation: $rCTb = KT/6\pi\mu'D$, for bulk solution viscosity (μ') of 0.001 Pa.s at 20°C (T), K is Boltzmann constant and D is the obtained CTb diffusion. rCTb obtained of approximately 3.7 nm is in agreement to CTb radius previously reported.[5] Table S1 shows the results of lipid bilayers without GM1 showing non-specific interaction to lipid bilayers containing sphingomyelin and cholesterol.

Table S1: Resistance and capacitance data for MSLBs at a fixed concentration (40 nM) of CTxB. Results presented reflect the change (Δ) recorded following CTb addition, relative to bilayer prior to CTb interaction and the non-specific adsorption to the lipid membrane was evaluated in the presence of sphingomyelin and cholesterol.

Lipid composition	ΔR (kΩcm^2)	ΔC (μF/cm^2)	Slow CTb ($\mu m^2 . s^{-1}$)	Pop (%)
Sym DOPC	0.05±0.01	-0.4±0.01	11.12 ± 2.51	65
sym DOPC/SM/Chol (2:2:1)	0.66±0.02	-1.3±0.12	1.50 ± 0.20	80

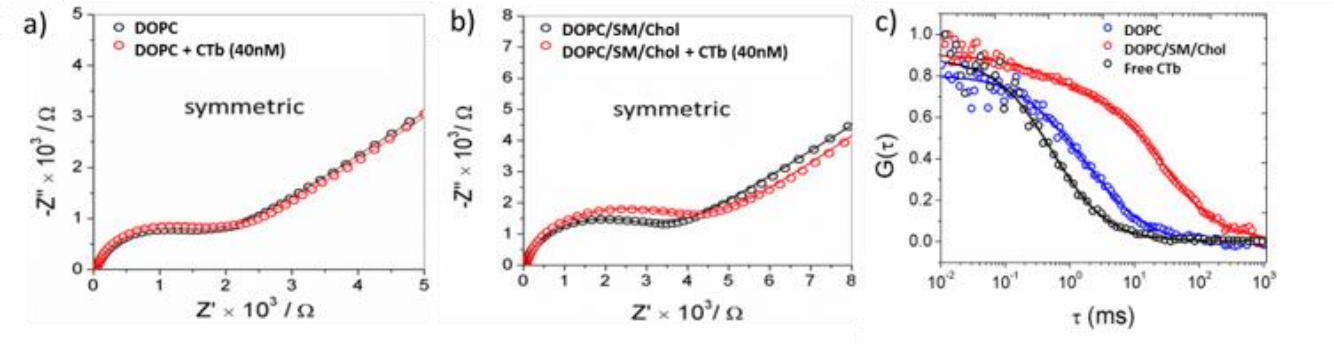

Figure S5. Electrochemical impedance spectra for microcavity array based supported lipid bilayers on gold electrodes with (red) and without (black) the presence of CTb. a) Illustrates EIS data of symmetric DOPC bilayers with and without CTb. b) Represents the respective EIS data without the presence of CTb for symmetric raft-composition bilayers comprised of DOPC/SM/Chol (2:2:1) (mol/mol/mol). The EIS data are recorded in the presence of 1 mM $[Fe(CN)_6]^{3-/4-}$ internal redox probe in 0.1 M KCl electrolyte solution in PBS buffer at the potential of +0.26 V vs. Ag/AgCl (1 M KCl). c) Shows the ACF curves obtained for free diffusion CTb-A555 in PBS (pH 7.4) (black circles), at the membrane surface of symmetric DOPC lipid bilayers (blue circles) and DOPC/SM/Chol (2:2:1) (mol/mol/mol) (red circles).

Fluorescence Lifetime Spectroscopy (FLIM) of bound CTb

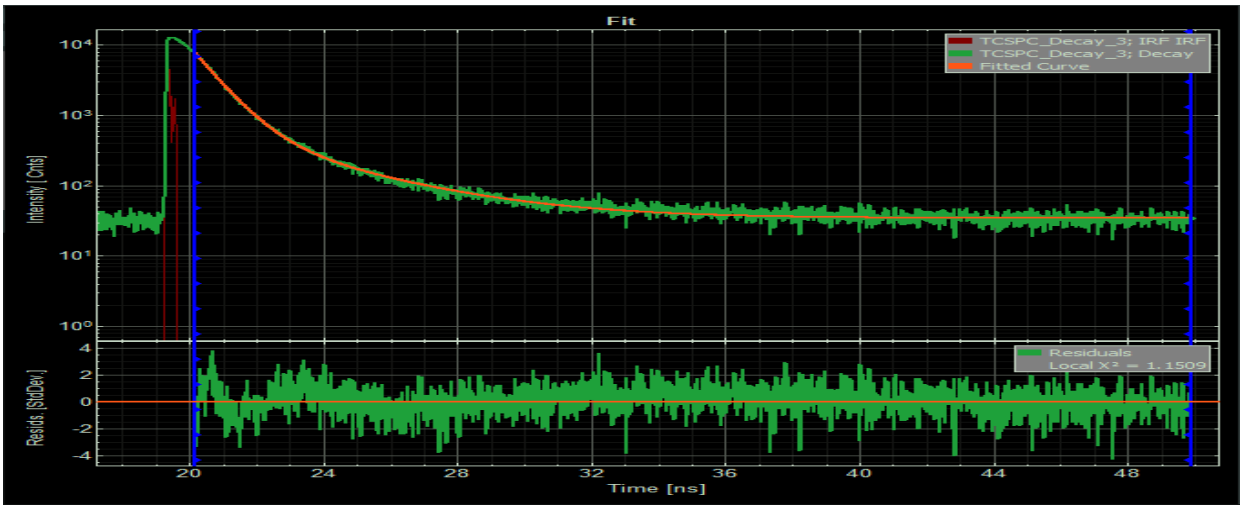

Figure S6. Fluorescent lifetime imaging decay of labelled CTb-Alexa555 for composition DOPC/SM/Chol (4:4:2 mol %) + GM1 (1 mol %).

Table S2. Fluorescence lifetime of CTb-A555 after binding to GM 1 in asymmetric and symmetric lipid bilayers.

	Ex/Em	Asym DOPC + GM1 (1 mol%)		Asym DOPC/SM/Chol (2:2:1) + GM1 (1 mol%)		Asym DOPC/SM (1:1) + GM1 (1 mol%)		Sym DOPC/SM/Chol 2:2:1 + GM1 (1 mol%)		Sym DOPC/SM (1:1) + GM1 (1 mol%)	
	λ (nm)	τ (ns)	τ_{Amp} (%)	τ (ns)	τ_{Amp} (%)	τ (ns)	τ_{Amp} (%)	τ (ns)	τ_{Amp} (%)	τ (ns)	τ_{Amp} (%)
CTb-A555	555/580	τ_1 = 3.12 τ_2 = 0.67	20 80	τ_1 = 2.71 τ_2 = 0.77	23 77	τ_1 = 3.00 τ_2 = 0.74	20 80	τ_1 = 2.84 τ_2 = 0.78	16 84	τ_1 = 3.34 τ_2 = 1.03	26 74

Table S3. Lateral diffusion of labeled CTb-A555 and population of fast and slow diffusing against CTb unlabelled concentration. The asymmetric lipid bilayers comprised of DOPC +GM1 with 1mol% and 5%mol% of GM1 in the distal leaflet.

Distal leaflet composition	CTb (nM)	$D_{CTb}(\mu m^2 s^{-1})$	Population CTb		Number of molecules CTb (N_{CTb})
		D_{CTb} fast	$\%P_{CTb}$ fast	$\%P_{CTb}$ slow	
DOPC + 1% (mol) GM1	4	5.23 ± 3.29	100	-	5.54 ± 4.09
	10	4.43 ± 1.46	67.1 ± 24.3	32.9 ± 23.3	4.46 ± 1.51
	40	4.74 ± 0.89	28.3 ± 14.5	71.7 ± 14.4	5.34 ± 2.47
	80	2.51 ± 0.79	5.7 ± 2.3	94.3 ± 2.3	2.69 ± 1.12
DOPC + 5% (mol) GM1	4	8.18 ± 1.75	100	-	4.43 ± 1.13
	10	5.30 ± 1.09	100	-	5.07 ± 1.41
	20	4.72 ± 1.16	89.2 ± 1.2	10.8 ± 1.2	7.59 ± 2.02
	40	2.36 ± 1.12	8.2 ± 5.7	91.8 ± 5.7	4.02 ± 1.15
	80	1.93 ± 0.69	9.7 ± 8.9	90.2 ± 5.6	3.34 ± 1.98

Table S4. Lateral diffusion of labelled CTb-A555 and population of fast and slow diffusing against CTb unlabelled concentration. The asymmetric lipid bilayers comprised of DOPC/SM (1:1) (mol/mol) + GM1 with 1 mol% and 5 mol% of GM1 in the distal leaflet shown the effect of SM containing membrane in CTb diffusion within CTb concentration.

Distal leaflet composition	CTb (nM)	D_{CTb} ($\mu m^2.s^{-1}$) Population CTb			Number of molecules CTb (N_{CTb})	D_{DOPE} ($\mu m^2.s^{-1}$)
		D_{CTb} fast	$\%P_{CTb}$ fast	$\%P_{CTb}$ slow		
DOPC/SM (1:1) + 1% (mol) GM1	4	1.76 ± 0.64	54 ± 27	55 ± 31	7.28 ± 2.67	5.4 ± 1.1
	10	1.10 ± 0.97	29 ± 26	71 ± 26	4.47 ± 3.81	5.0 ± 0.9
	20	0.87 ± 0.43	23 ± 25	77 ± 25	8.44 ± 7.31	4.0 ± 0.7
	40	0.36 ± 0.37	19 ± 19	81 ± 19	4.38 ± 3.37	2.0 ± 0.8
DOPC/SM (1:1) + 5% (mol) GM1	4	0.60 ± 0.19	36 ± 29	64 ± 29	4.86 ± 3.45	5.3 ± 1.0
	10	0.41 ± 0.21	18 ± 8	88 ± 12	3.21 ± 2.16	4.3 ± 1.1
	20	0.20 ± 0.29	7 ± 11	95 ± 5	3.13 ± 1.87	2.4 ± 0.4

References

(1) Mallon, C. T.; Jose, B.; Forster, R. J.; Keyes, T. E. Protein Nanopatterning and Release from Gold Nano-Cavity Arrays. *Chem. Commun.* **2010**, *46* (1), 106–108. https://doi.org/10.1039/B919352A.

(2) Adamson, K.; Spain, E.; Prendergast, U.; Moran, N.; Forster, R. J.; Keyes, T. E. Peptide-Mediated Platelet Capture at Gold Micropore Arrays. *ACS Appl Mater Interfaces* **2016**, *8* (47), 32189–32201. https://doi.org/10.1021/acsami.6b11137.

(3) Jose, B.; Mallon, C. T.; Forster, R. J.; Blackledge, C.; Keyes, T. E. Lipid Bilayer Assembly at a Gold Nanocavity Array. *Chem. Commun.* **2011**, *47* (46), 12530–12532. https://doi.org/10.1039/C1CC15709D.

(4) Müller, C. B.; Loman, A.; Pacheco, V.; Koberling, F.; Willbold, D.; Richtering, W.; Enderlein, J. Precise Measurement of Diffusion by Multi-Color Dual-Focus Fluorescence Correlation Spectroscopy. *EPL (Europhysics Letters)* **2008**, *83* (4), 46001. https://doi.org/10.1209/0295-5075/83/46001.

(5) Miller, C. E.; Majewski, J.; Watkins, E. B.; Weygand, M.; Kuhl, T. L. Part II: Diffraction from Two-Dimensional Cholera Toxin Crystals Bound to Their Receptors in a Lipid Monolayer. *Biophysical Journal* **2008**, *95* (2), 641–647. https://doi.org/10.1529/biophysj.107.120808.